Hydrogen-Bond Interactions in Organically-Modified Polysiloxane Networks Studied by 1D and 2D CRAMPS and Double-Quantum ^{1}H MAS NMR

Jiří Brus* and Jiří Dybal

Institute of Macromolecular Chemistry, Academy of Sciences of the Czech Republic, 162 06 Prague 6, Czech Republic

Received March 18, 2002

ABSTRACT: Hydrogen-bonding interactions, distribution of various hydroxy groups, and surface morphology in organically modified polysiloxane networks were studied by solid-state NMR techniques based on ^{1}H spin-exchange, double-quantum, and ^{1}H−^{29}Si heteronuclear MAS NMR spectroscopy. ^{1}H CRAMPS experiments revealed four main types of OH groups differing in hydrogen-bond strength, order, and dynamics, which are mutually dipolar-coupled (their interatomic distances are not larger than 0.5 nm), however, not involved in fast chemical exchange even in the fully hydrated state at room temperature. The resulting hydrogen-bonding network is inhomogeneous in the entire set of hydroxyl groups. These findings were correlated with the quantum chemical geometry optimization of hydrogen-bonded local structures and subsequent calculations of ^{1}H NMR chemical shifts. 2D ^{1}H spin-diffusion experiments were used to determine the ^{1}H−^{1}H interatomic distances and to probe the average size of OH clusters, which is ca. 1−2 nm. Intimate mixing of strongly hydrogen-bonded OH and methyl groups was confirmed by 2D double-quantum ^{1}H MAS NMR spectra. Hydrogen-bonding strength of various hydroxyl clusters was evaluated with respect to the type of siloxane structure units and geometry of the siloxane matrix by 2D ^{1}H−^{29}Si heteronuclear experiments.

Introduction

Polysiloxane and polysilsesquioxane networks are short-range-ordered materials intermediate between completely crystalline cristobalite and the least ordered silicate glasses.[1,2] The arrangement of silanol groups, formation and structure of the hydrogen-bonding network, and location of mobile water molecules determine chemical and physical properties of these networks. It is well-known that the reactivity and the use of silica as well as modified siloxane networks are among others intrinsically linked to the presence, quantity, structural environment, and behavior of hydroxyl (OH) groups. These groups are classified according to their hydrogen bonding, their coordination to silicon, and their communication or accessibility to water. Out of various techniques, ^{1}H NMR is the most useful because of its high sensitivity to hydrogen bond strength.[1−8] Using fast MAS[2,3,5,6,9] or CRAMPS (combined rotation and multipulse spectroscopy)[2−4,8] techniques, the homogeneous line broadening is removed, and resulting spectra are well resolved and can be interpreted in view of basic structure units. However, so far mainly basic silica products prepared by sol−gel polycondensation of tetraethoxysilane (TEOS) or by flame hydrolysis of $SiCl_4$ have been studied by these methods,[1−6,8,10−18] although modified siloxane materials are of general interest.[9,19−27] Up to the present time, predominantly chemical homogeneity (spatial proximity of various siloxane or monomer units) of organically modified networks was studied by 2D solid-state NMR techniques.[25−27] It was found that these materials are more or less homogeneous; however, variability in hydrogen-bonding strength and hydroxyl cluster formation was not studied.

* Corresponding author. Telephone: +420 2 20403380. Fax: +420−2−3535981. E-mail: brus@imc.cas.cz.

In this paper, we focused our attention on hydrogen-bonding properties of OH protons and their local arrangement in organically modified siloxane networks. For these purposes, we used solid-state NMR techniques based on fast ^{1}H MAS, CRAMPS, spin-diffusion, double-quantum, and FSLG (frequency-switched Lee−Goldburg decoupling) heteronuclear experiments as well as quantum chemical (DFT: density functional theory) calculations. We present here an attempt to describe the arrangement of Si−OH groups and water molecules with respect to local structures of basic types of silica networks.

Experimental Section

Preparation of Siloxane Materials. Siloxane materials were prepared by acid-catalyzed sol−gel polycondensation of mixtures, the composition of which is listed in Table 1. A solution of hydrochloric acid was added to a mixture of alkoxysilanes with ethanol. The resulting mixture (ca. 10 g) was stirred for 30 min and subsequently poured onto a Petri dish (5.5 cm in diameter). Polycondensation then took place under laboratory conditions. After a year, the products were finely powdered and placed into an air-conditioned box (relative humidity (RH) = 55%; t = 25 °C) for 1 month. Partially deuterated samples were obtained by simple exchange with deuterium oxide at laboratory temperature and pressure in a closed vessel containing a dish with D_2O. After the deuteration procedure, the samples were not subsequently dried. Deuterium exchange periods were 24 or 48 h.

NMR Spectroscopy. NMR spectra were measured by using a Bruker DSX 200 NMR spectrometer in 4 and 7 mm ZrO_2 rotors at frequencies 39.75 and 200.14 MHz (^{29}Si and ^{1}H, respectively). For acquisition of ^{1}H MAS NMR spectra, the spinning frequency was 16−18 kHz and the strength of the B_1 field 62.5 kHz (π/2 pulse 4 μs). 1D CRAMPS spectra at slow MAS (2 kHz) were acquired using BR-24 pulse sequence.[28] The 2D spin-exchange experiment proposed by Caravatti et al.[29] was used to observe ^{1}H−^{1}H correlation. In direct and indirect detection periods, the BR24 pulse sequence was used. Spin-

10.1021/ma0204249 CCC: $22.00 © 2002 American Chemical Society
Published on Web 12/05/2002

Table 1. Composition of Reaction Mixtures[d]

no.		mole ratio	code
1	TEOS[a]/C_2H_5OH[c]/H_2O/HCl	1/4.50/3/0.03	**TE**
2	TEOS/DMDEOS[b]/C_2H_5OH/H_2O/HCl	0.75/0.25/4.50/3/0.03	**TE-DM 3−1**

[a] TEOS (tetraethoxysilane): Synthesia Kolín, Czech Republic. [b] DMDEOS (dimethyldiethoxysilane): Wacker-Chemie GmbH., Germany. [c] Ethanol, 0.1% w/w water: Merck, Germany. [d] Partially deuterated samples are referred to as **TE-D_2O**.

diffusion mixing time varied from 0.1 to 40 ms. Intensity of the B_1 field was 140 kHz ($\pi/2$ pulse 1.8 μs), and small and large windows were 1.0 and 3.8 μs, respectively. The ^{1}H scale was calibrated with an external standard—glycine (low-field NH_3^+ signal at 8.0 ppm and the high field α-H signal at 2.8 ppm). 2D ^{1}H−^{29}Si heteronuclear correlation spectra were obtained with a pulse sequence proposed by de Groot et al.[30] with frequency-switched Lee−Goldburg ^{1}H−^{1}H decoupling at 83 kHz, with ^{1}H resonance offset −53.4 kHz and +64.6 kHz. MAS frequency was 7 kHz and TPPM heteronuclear decoupling at 62.5 kHz was used. ^{1}H double-quantum-filtered (DQF) spectra were measured applying Levitt's C7 pulse sequence[31] at MAS frequency 10224 Hz and B_1 strength 83 kHz ($\pi/2$ pulse 3.1 μs).

Ab Initio Calculation of Molecular Structures and ^{1}H NMR Chemical Shifts. The calculations were performed using the Gaussian 98 program package.[32] Molecular geometries were fully optimized at the DFT (B3LYP functional[33]) level, the basis set being of 6-31G(d) quality. The gauge-including atomic orbitals (GIAO) method[34,35] was employed to calculate absolute shielding constants (σ, ppm) for proposed structure units. Subtraction gave the calculated chemical shift (δ, ppm) of the structures relative to TMS. The basis set of 6-311+G(2d,p) quality was used in computation of ^{1}H NMR shifts.

Results and Discussion

Quantity and Quality of Hydroxyl Groups. It is generally accepted that there are three main types of OH protons in silica gels. Physisorbed water and labile, rapidly exchanging weakly hydrogen-bonded hydroxy groups are characterized by signals at ca. 5.0−3.0 ppm. Silanol protons in a variety of hydrogen-bonding environments are reflected by the broad peak ranging from 8 to 2 ppm, and non-hydrogen-bonded silanols correspond to the sharp peak at ca. 1.8−1.2 ppm.[2−8]

In contrast to the previous statements,[2,3,8] four basic types of hydroxyl groups were detected in CRAMPS spectrum even in hydrated silica gel **TE** (Figure 1): strongly hydrogen-bonded (s-HB OH) and weakly hydrogen-bonded hydroxyl groups (w-HB OH), physisorbed water (p-H_2O) and non-hydrogen-bonded silanols (n-HB OH) at 7.0, 4.3, 5.2, and 1.4 ppm, respectively. The non-hydrogen-bonded silanols (1.4 ppm; ca. 10% of all protons) were previously found before dehydration of samples only in fumed[3] and pyrogenic silica,[5] but not in silica gel prepared by the sol−gel process. In fumed silica, these isolated silanols were attributed to interparticle water-inaccessible silanols, which are located at a point of contact between two or more particles. The above-mentioned findings reflect huge structural variability of silica gels prepared by the sol−gel process under various conditions.

Relatively good resolution in spectra excludes extensive conformation changes leading to variation in hydrogen-bonding strength and/or chemical exchange between the sites with correlation frequency exceeding tens of hertz, because faster dynamics processes would significantly broaden the signals in ^{1}H CRAMPS spectra. However, as the signals are not completely separated and resolved, some portion of dynamic changes in hydrogen-bond strength is possible. To obtain deeper

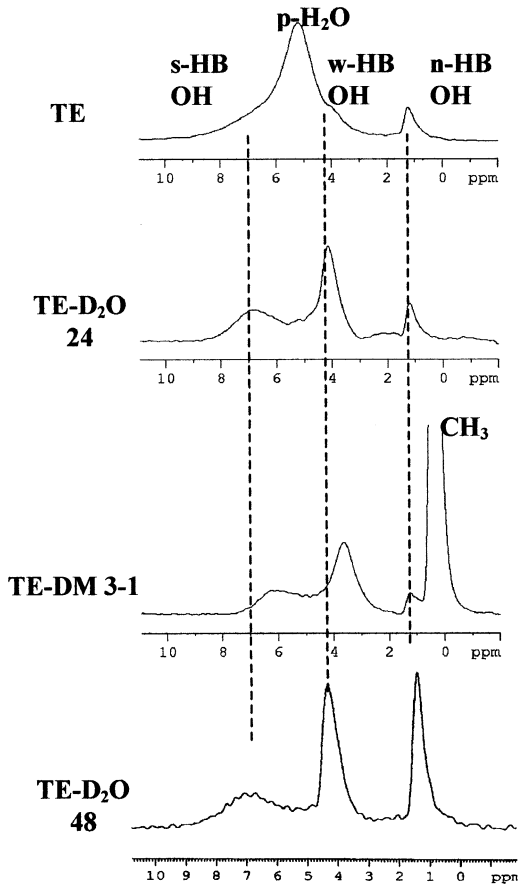

Figure 1. ^{1}H CRAMPS NMR spectra of siloxane networks **TE**, **TE-D_2O**, and **TE-DM 3-1**. (Numbers 24 and 48 indicate time in hours of deuterium exchange of the **TE** system.)

information about possible chemical exchange we performed variable-temperature experiments during which we observed changes in ^{1}H NMR chemical shifts of signals s-HB, w-HB, and n-HB silanols. The signal of s-HB OH moves toward the higher field with increasing temperature as a result of effective weakening of hydrogen bonds. The position of the signal reflecting w-HB OH very slightly moves oppositely toward lower field. This indicates an increasing rate of chemical exchange with increasing temperature. As we did not observe extensive coalescence of the signals, these results confirm our prediction that the rate of chemical exchange between different sites is not large, and effectively only a fraction of hydroxyl protons located at the boundary of various clusters is involved in this process at room temperature.

Better resolution of CRAMPS spectra compared with MAS only (i.e., narrowing of signal of s-HB OH in **TE**) reflects slow molecular motion of these protons. The correlation frequency of dominant motion has to be as small as 12 kHz, i.e., five times smaller than subcycle time t_c^{-1} of BR24 consisting of four pulses and delays that average the dominant zero-order term of dipolar Hamiltonian. Higher correlation frequency would lead

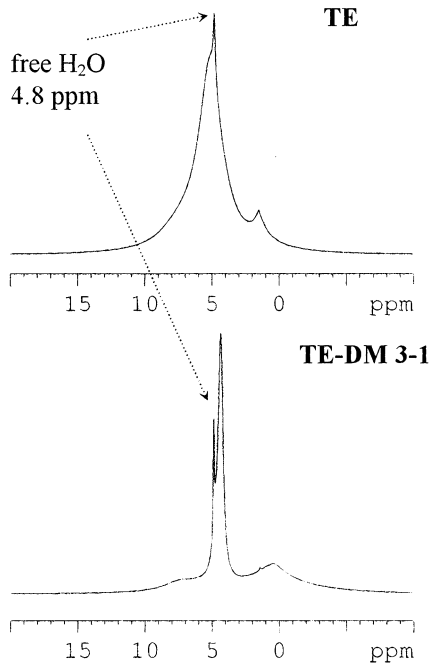

Figure 2. ^{1}H MAS NMR spectra of fully hydrated **TE** silica gel and **TE-DM 3-1** network. (Hydration was performed at RH = 100% over 24 h.)

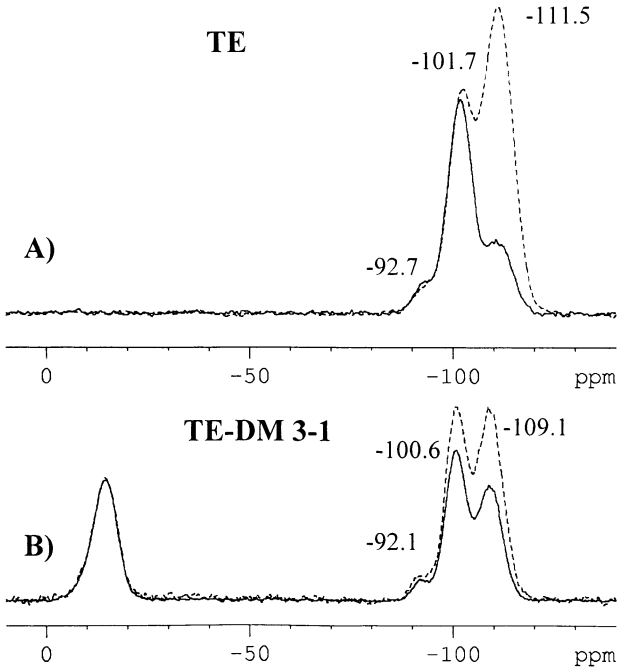

Figure 3. ^{29}Si MAS (dashed line) and ^{29}Si CP/MAS (solid line) NMR spectra of siloxane systems **TE** and **TE-DM 3-1 (**A and B, respectively).

to the destructive interference and signal broadening. On the other hand, physisorbed water at 5.2 ppm and labile weakly hydrogen-bonded hydroxyls are more mobile (correlation frequency $\gg$ 60 kHz).[2] Nevertheless, partial narrowing of the signal by applying BR24 or fast MAS accompanied by formation of weak spinning sidebands indicates residual dipolar interactions. This fact and the downfield shift of the physisorbed water resonating at 5.2 ppm compared with the signal of free condensed water (signal at 4.8 ppm; see Figure 2) indicate modification of H-bond strength as the result of a certain degree of ordering and restriction of molecular motion. We assume that physically adsorbed water fills suitable pores in which the surface structures of siloxane network are partially and temporarily retained in a bulk of water. Water molecules move from the layer directly and strongly interacting with surface silanols into an inner part of a drop where water−water intermolecular interactions and liquidlike behavior dominate. Molecular motion, i.e., chemical exchange, between these "sites" averages the strength of hydrogen bonds of water molecules, thus leading to an average value of chemical shifts. We believe that this signal at ca. 5.2 ppm reflects large clusters of water molecules which are mutually hydrogen bonded and also interact with the surface silanols.

Well-resolved signals in CRAMPS spectra of partially deuterated network **TE-D_2O** obtained from **TE** by partial exchange with D_2O clearly reflect a limited structural variation of strongly and weakly hydrogen-bonded OH's. As these NMR signals can be considered as distribution curves reflecting the strength of hydrogen bonds, it is quite clear that systems of hydrogen interactions is neither quite homogeneous and uniform nor quite random. Instead, both types of hydroxyl groups comprising ca. 20% and 31% of all protons in the system, respectively, form several structures or ordered areas with different most probable lengths of hydrogen bonds. Physisorbed water (ca. 39% of all protons) occupying pores easily accessible to the water vapor was exchanged by D_2O with no effort. However, the exchange of strongly and weakly hydrogen-bonded hydroxyls with D_2O is much slower (see Figure 1).

Table 2. Composition of Prepared Siloxane Networks Expressed as Mole Fraction of D^n and Q^n Structure Units; Total Degree of Condensation[a], q_t; the Number of Silanols per Silicon Atom; Fraction of Proton-Inaccessible Siloxane Silicon Atoms[b], Δn_q; the Amount of Water (Δm_{H_2O}) Defined as a Weight Loss after Heating of Samples at 180° C, for 2 h

code	mole fraction D^2	Q^2	Q^3	Q^4	q_t	SiOH/Si	Δn_q, mol %	Δm_{H_2O}, wt %
TE		0.03	0.37	0.60	0.89	0.43	32	8.8
TE-DM 3-1	0.25	0.03	0.32	0.40	0.90	0.36	18	7.8

[a] $q_t = [\sum_{n=1}^{2} nD^n]/2 + [\sum_{n=1}^{4} nQ^n]/4$. [b] Fraction of proton-inaccessible part of the siloxane networks was determined from quantitative analysis of ^{29}Si MAS NMR spectra and from their comparison with ^{29}Si CP/MAS NMR spectra compensated for differences in CP dynamics and $T_{1\rho}$ (^{1}H) relaxation; experimental details and discussion are introduced in our previous work.[24]

The absence of physisorbed water at 5.2 ppm suggests that large clusters of water molecules do not interact with the surface of **TE-DM 3-1** material. Instead interaction of isolated water molecules or their small clusters is supposed. Although this physisorbed water is absent in the **TE-DM 3-1** system, the mutual mole ratio of other hydroxy groups is almost the same in both materials (s-HB/w-HB/n-HB = 20/28/5). On the basis of quantitative analysis of ^{1}H CRAMPS spectra and from the known condensation rate of siloxane structure units (0.90) and number of silanol groups per silicon atom (0.36) determined from ^{29}Si MAS NMR spectra[24] (see Figure 3) we calculated the fraction of water molecules involved in hydroxyl clusters in the **TE-DM 3-1** network. On average, there are two molecules of H_2O per three silanol groups in the clusters. Quantitative data are summarized in Table 2.

The presence of methyl substituents in the modified network moves chemical shifts of signals of both strongly and weakly hydrogen-bonded hydroxyls toward the

higher field, while the signal of non-hydrogen-bonded silanol is not affected. The unaffected frequency of this signal indicates that direct inductive effects of methyl units perturbing electron density are too small to affect ^{1}H NMR chemical shifts. From this follows that the observed upfield shifts of strongly and weakly hydrogen-bonded OH's correspond to the decrease in the hydrogen-bond strength as reflected by an increase in H···O (r_{HB}) and O···O (d_{OO}) distances, calculated using the following relations:[36−38]

$$\delta_{iso}(\text{ppm}) = \frac{4.65}{r_{HB}(\text{nm})} - 17.4 \qquad (1)$$

$$\delta_{iso}(\text{ppm}) = 79.05 - 255 d_{OO}(\text{nm}) \qquad (2)$$

Strongly and weakly hydrogen-bonded OH's in **TE** network are characterized by hydrogen bond lengths r_{HB} = 0.176−0.203 and 0.207−0.227 nm and d_{OO} = 0.275−0.288 and 0.290−0.298 nm, respectively. In copolymer siloxane networks **TE-DM 3-1**, both these distances are larger: r_{HB} = 0.190−0.207 and 0.219−239 nm, and d_{OO} = 0.282−0.290 and 0.292−0.302 nm. These empirically predicted results correspond quite well with quantum chemical (DFT) calculations discussed in detail later.

Local Silanol Structures: Quantum Chemical Calculation of ^{1}H NMR Chemical Shifts. Quantum-chemical geometry optimization and subsequent calculation of ^{1}H NMR chemical shifts of several proposed structures (see Figure 4) was used to obtain deeper insight into local structures of hydrogen bonds. In all the clusters, the dangling bonds have been saturated with hydrogen atoms. Thus, −Si−H_3 structure units constitute ending groups of model clusters. Although there is a small systematic deviation of ab initio calculated chemical shifts from those empirically predicted for various hydrogen bond lengths according to eqs 1 and 2, the main trends are the same (see Figure 5). This shows that ab initio calculations of ^{1}H NMR chemical shifts at this level are precise enough to provide direct structural information. The obtained results prove reliability of the optimized model structures, confirming that an increasing number of water molecules in the systems leads to an increase in hydrogen bond strength and, consequently, to the low-field shift of ^{1}H NMR signals. The most deshielded are OH protons hydrogen-bonded to water involved in the hydrogen-bonding network. In accord with the experimental results, the ^{1}H NMR chemical shift of non-hydrogen-bonded silanols is not affected by the presence of methyl groups in the model systems. On the contrary, in the vicinity of methyl units, the hydrogen-bonding strength is weakened; however, the replacement of silanol sites by methyls does not completely destroy the formation of hydrogen-bonding network. As follows from our calculations (see Figure 4), all types of various hydroxyls can be mutually very close. However, in the case of intimate mixing of different types of OH groups, small changes of conformations and/or motion of water molecules would lead to significant variation of hydrogen-bonding strength and thus to severe broadening of the ^{1}H NMR signals. Therefore, we instead suggest the presence of relatively large clusters with more or less uniformly arranged OH groups in the systems. Protons within these regions can be involved in dynamic processes and thus the resulting ^{1}H NMR chemical shifts would reflect the average geometry and average hydrogen-bonding strength within the cluster. Although the dynamic processes involving OH hydrogen atoms at the boundary are possible, their extent is not significant. This is confirmed by variable-temperature experiments during which we observed changes in the ^{1}H NMR chemical shifts of signals s-HB, w-HB, and n-HB for silanols. As all signals move toward higher field with increasing temperature as a result of the weakening of hydrogen bonds and because we did not observe exten-

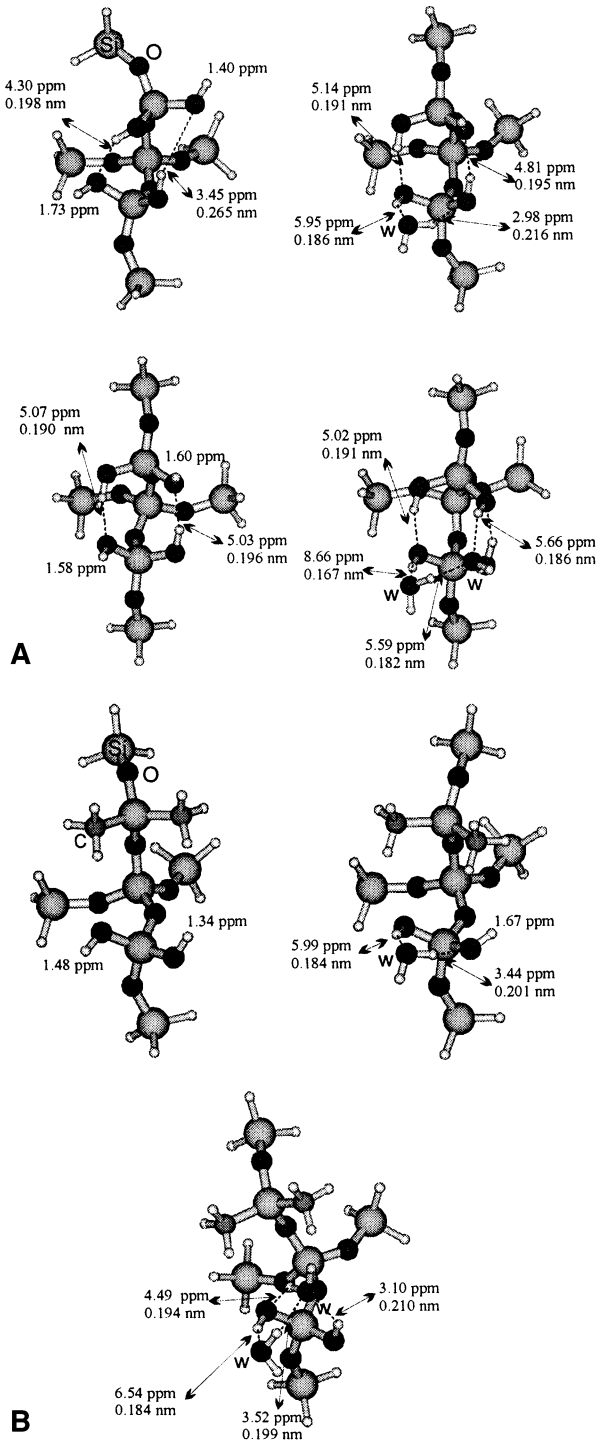

Figure 4. Geometry-optimized model structures **TE** (A) and **TE-DM 3-1** (B) networks, respectively. Hydrogen bond distances r_{HB} and corresponding ^{1}H NMR chemical shifts of OH protons calculated by quantum-mechanics (DFT) calculations are also listed. In all the clusters, the dangling bonds have been saturated with hydrogen atoms.

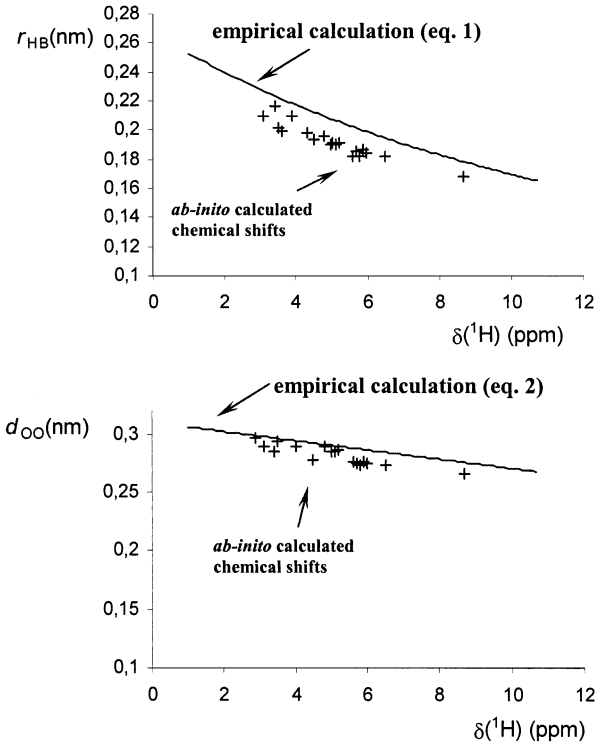

Figure 5. Dependence of hydrogen bond distance r_{HB} and d_{OO} vs ^{1}H NMR chemical shift calculated from eq 1 and 2 (solid lines). Dots represent ab initio calculated data.

sive coalescence of the signals, these results confirm small rate of chemical exchange between different sites.

On the other hand, individual types of OH groups can be truly separated from each other, thus preventing chemical exchange. To obtain detailed information about distribution of these various hydroxyls, we performed 2D ^{1}H−^{1}H correlation experiment based on spin exchange.

Hydrogen-Bond Network: 2D CRAMPS and ^{1}H−^{29}Si FSLG HETCOR. Although the spin-exchange experiment without multipulse averaging of ^{1}H−^{1}H dipolar interactions were performed on several siloxane and silicate materials at high spinning speed,[25−27,39,40] the obtained data were only qualitatively analyzed. Quantitative analysis was highly complicated by intensive spinning sidebands or lower resolution (broad wings of signals) and/or weakening of dipolar couplings leading to long mixing times. Therefore, we applied the 2D spin-exchange experiment proposed by Caravatti et al.[29] originally used for the analysis of polymer blends. In this experiment, mutually dipolar coupled hydrogen atoms differing in chemical shifts produce off-diagonal cross-peaks. (Interatomic distance between them has to be less than ca. 0.5 nm, otherwise off-diagonal signals do not evolve.) The dependence of the cross-peak intensity on mixing time reflects their interatomic distance. For instance, in highly rigid organic solids (e.g., glycine) equilibrium signal intensity correlating α-H and NH_3^+ protons is achieved during ca. 300 μs.[41] On the other hand, in heterogeneous systems like polymer blends, evolution of cross-peak intensity instead reflects relayed polarization transfer and thus the size of the domains of both components. In well-miscible systems, which are composed of small size domains, equilibration can be achieved during several milliseconds. In heterogeneous systems, equilibration requires tens to hundreds of milliseconds.

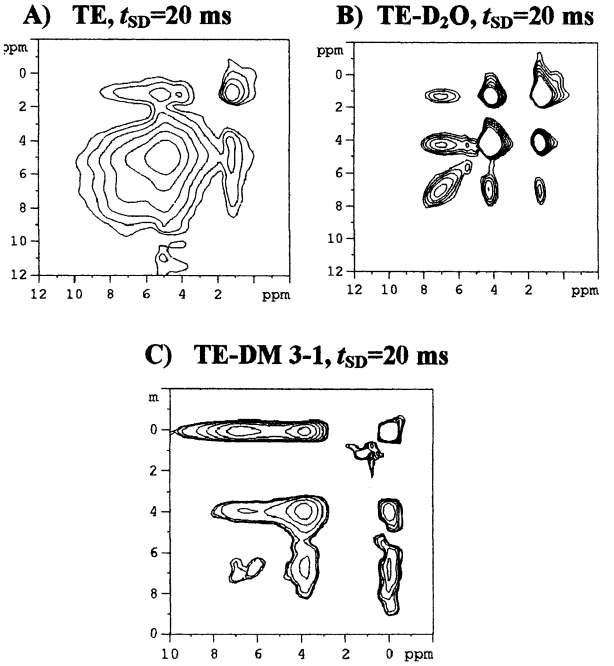

Figure 6. 2D ^{1}H spin-exchange CRAMPS spectra of **TE** (A), **TE-D$_2$O** (B), and **TE-DM 3-1** (C) systems, respectively, measured at 20 ms spin-diffusion mixing time.

Even though it is generally accepted that silanols reflected by the signal at 1.4 ppm are isolated and "water-inaccessible", the appearance of the cross-peak correlating to 5.2 ppm clearly proves dipolar interaction and the spin exchange between these silanols and physisorbed water (see Figure 6A). The distance of these silanols and water molecules is smaller than 0.4 nm. These silanols are probably entrapped in cages with a neck diameter of 0.28 nm, which corresponds to the effective diameter of a water molecule.

As followed from the equilibrium intensity of off-diagonal cross-peaks, it is quite clear that the vast majority of all hydrogen atoms in all three studied systems are in close contact, and the average ^{1}H−^{1}H distance between them is smaller than 0.5 nm. More accurate quantitative data can be derived from simulation of the whole spin-diffusion process. This simulation can be performed according to the procedure described in the literature[42,43] for a general two-component system with an interface and variable diffusivity and dimensionality ($\epsilon = 1,2,3$), which we have used in our previous studies of polymer blends[44] and copolymers.[45] In contrast to polymer blends or copolymers in which each component is well-defined, in the case of hydroxyl clusters, we have to use a wide range of approximations. Because of this fact our analysis of spin-exchange (spin-diffusion) process can lead to only a rough determination of surface morphology, because the structure and composition of the siloxane network surface are not well-defined.

Although the studied systems consist at least of three phases, the evolution of individual cross-peak intensities can be considered as spin-diffusion dependence for two-phase system with an interface. Each cross-peak correlates two phases (A and B), and if these two phases are separated by the third phase C, then C can be considered as an interface. In addition, the presence of an interface could reflect OH protons at the boundary taking part in mutual exchange or other dynamic process. In our model, we assume that spin exchange

Table 3. Calculated Spin-Diffusion Coefficients, *D*, and Corresponding Transverse Relaxation Time, T_2

system	hydroxyl type	T_2, ms	D,[a] nm^2·ms^{-1}
TE	p-H_2O	0.55	0.05
	s-HB OH	0.45	0.06
	w-HB OH	1.70	0.02
	n-HB OH	20.0	0.001
TE-DM 3-1	s-HB OH	0.60	0.05
	w-HB OH	1.80	0.02
	$-CH_3$	0.25	0.11

[a] Calculated by Assink's method[46] $D_{eff} = [2(r_0)^2]/(T_2)$, where r_0 is van der Waals radius.

occurs in proton-rich domains, which are formed by surface silanols and adsorbed water molecules. As neat silica is generally highly porous material with surface area ca. 350−450 m^2·g^{-1}, proton-rich domains can form more or less continuouslyum within the whole material, especially in the case of organically modified network containing $(CH_3)_2Si-$ units. The (111) and (100) plains of the β-cristobalite crystal structure have been proposed previously as useful models for segments of the silica surface.[1] Also liquid water is often considered to have pseudocrystalline structure. This means that the hydrated surface is formed by segments of the short-range ordered silanol groups and water molecules bound into a hydrogen-bonded network. These surface segments cannot be very large (smaller than 10^3 atoms); otherwise, certain diffraction patterns would be manifested in the X-ray diffraction experiments.[1] Quantification of the length scale critically relies on the estimation of the effective spin-exchange coefficient. Generally, this coefficient reflects the average strength of dipolar interactions, i.e., molecular mobility and average $^1H-^1H$ separation. The β-cristobalite model can accommodate a hydroxyl surface density ca. 5 OH/1 nm^2. In this model, each single silanol is surrounded by six equidistant (0.5 nm) single silanols. However, in the hydrated state involving adsorbed water molecules, hydroxyl density is substantially increased. The experimentally determined ratio is 0.7 (H_2O) to 1 (HO−Si). This means that hydroxyl surface density is ca. 12 OH/1 nm^2. Under such conditions, the average $^1H-^1H$ interatomic distance is much shorter in the range from 0.23 to 0.27 nm. This is very close to the average proton−proton distance in organic polymers (0.22−0.25 nm).[42] From this point, it follows that the spin-exchange coefficient can be estimated according to Assink's relation[46] from the ^1H T_2 relaxation constant measured under 2 kHz MAS conditions by a standard Hahn−echo pulse sequence. Because of the low resolution, the spectra signals were deconvoluted into separate lines, and for each line, the magnetization decay was analyzed. Spin diffusion coefficients, which are in a good accord with a recently published value for water domains in a paper,[47] as well as ^1H T_2 relaxation constants are listed in Table 3. Another parameter required for proper simulation is the proton density of water, $\rho^H_{H_2O} = \rho_{H_2O}\phi^H_{H_2O} = 0.11 \times 10^{-21}$ g·nm^{-3}, where $\rho_{H_2O} = 1$ g·cm^{-3} is water density and $\phi^H_{H_2O} = 0.11$ is the water proton fraction. The assumption that the arrangement of silanol protons and water molecules in the surface clusters is locally similar to the molecular arrangement of pure water is quite justifiable, and therefore, the proton density of the hydroxyl clusters (s-HB, w-HB, n-HB) can be kept constant. It has to be stressed that in the case of n-HB OH protons, this assumption provides only a crude approximation. To determine proton density in dimethylsiloxane units physical properties of linear high-molecular-weight poly(dimethylsiloxane) were used as sufficient model: $\rho_{PDMS}{}^H = \rho_{PDMS}\phi^H_{PDMS} = 0.97 \times 0.08 = 0.08 \times 10^{-21}$ g·nm^{-3}. Calculated diameters of the clusters are presented in Figure 7.

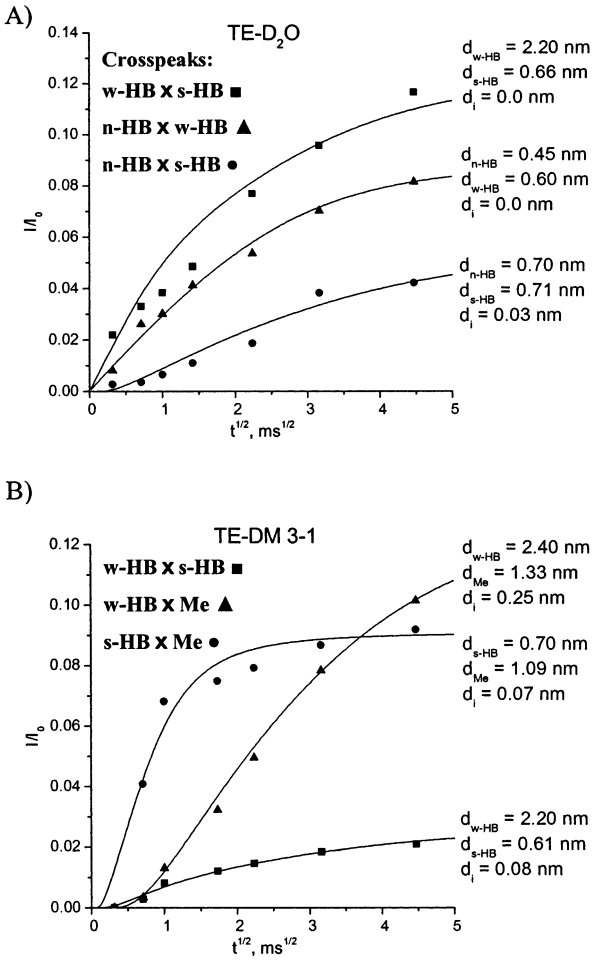

Figure 7. Experimental (dots) and simulated (lines) spin-diffusion curves, i.e., dependences of cross-peak intensity on mixing time. Dimensions of strongly, weakly and non-hydrogen-bonded hydroxyl clusters, methyl clusters and possible interfaces (d_{s-HB}, d_{w-HB}, d_{n-HB}, d_{Me} and d_i, respectively) calculated from individual spin-diffusion dependences are listed in each graph.

As follows from the rate and degree of equilibration of cross-peak intensities in the system **TE-D$_2$O**, the clusters of strongly and weakly hydrogen-bonded OH's form relatively large regions, and non-hydrogen-bonded silanols are dipolar-coupled with both types of these protons (see Figures 6 and 7). The almost undetectable volume of the interface following from the analysis of the spin-diffusion dependences indicates that all three types of OH's are probably in direct mutual contact, and the extent of chemical exchange and other dynamic processes involving boundary of hydroxyl clusters is not large. As cross-peak intensity correlating strongly and weakly hydrogen-bonded OH's does not tend to reach theoretical equilibrium intensity, the standard fitting of the spin-diffusion curve yields unrealistically large size of the weakly hydrogen-bonded clusters (>3 nm). Therefore, we suggest that a part of the weakly hydrogen-bonded OH protons (ca. 20%) is quite isolated. These isolated clusters occupy cavities, the distance of which to other protons is larger than ca. 0.5−0.6 nm. From the best fits (cf. Figure 7), employing our assumption

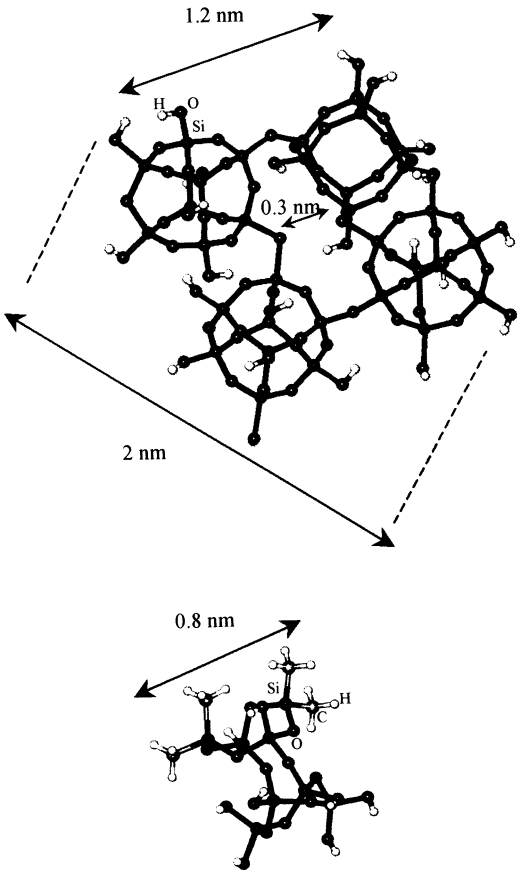

Figure 8. Idealized models of possible structures reflecting obtained interatomic distances. The upper structure corresponds to the cagelike model of **TE** system, while the lower one corresponds to **TE-DM 3-1** system.

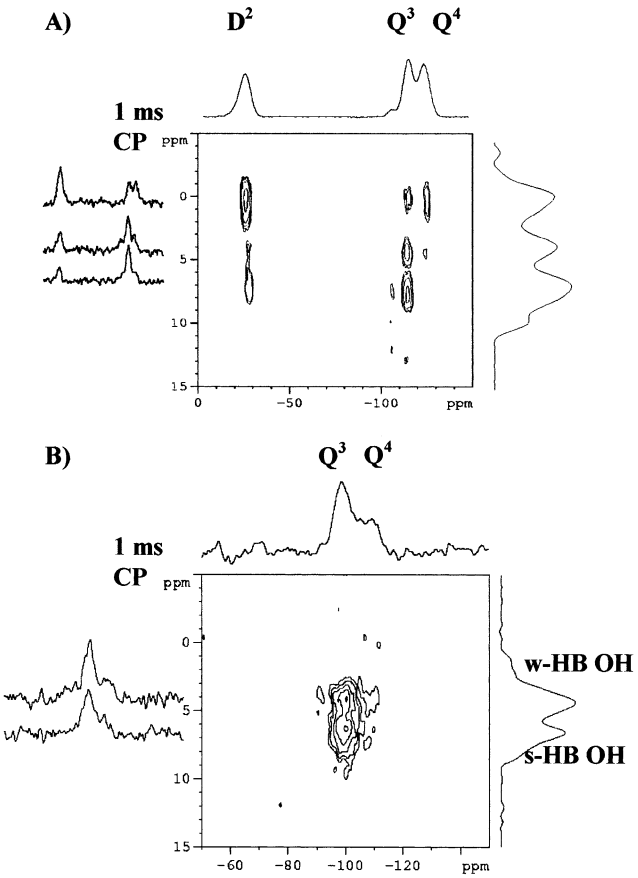

Figure 9. 2D $^{1}H-^{29}Si$ FSLG heteronuclear spectra of **TE-DM 3-1** (A) and **TE** (B) systems, respectively, and corresponding slices measured at 1 ms cross-polarization mixing time.

about main dimensionality ($\epsilon = 2$; at the surface, there are two possible directions for the magnetization diffusion) and dispersion of individual clusters (strongly hydrogen-bonded OH's are dispersed in weakly hydrogen-bonded OH's and non-hydrogen-bonded ≡SiOH's in strongly and/or weakly hydrogen-bonded OH), we estimated their average size. Although the obtained results are not entirely self-consistent, which originates from experimental errors (inaccuracy in integration of cross-peaks intensities) and from assumptions used in spin-diffusion analysis (regular repetition of the clusters, the same shape of the domains, and Gaussian distribution of their size, etc.), rough conclusions about the structure and morphology can be performed. It seems to be reasonable to conclude that weakly hydrogen-bonded OH's form the largest clusters with maximum diameter ca. 1.5−2.0 nm while clusters of strongly hydrogen-bonded OH's are smaller with diameter below 1.0 nm. The smallest size was obtained for non-hydrogen-bonded silanols (ca. 0.5−0.4 nm), indicating that they can be formed by two neighboring single silanols of Q^3 structure units, which are in an inappropriate geometry to form a hydrogen bond, and/or by two geminal silanols of the Q^2 structure unit, the maximum theoretical interatomic distance of which is about 0.4 nm. To have an idea about the dimension of hydroxyl clusters, the idealized cagelike structure of these networks is presented in Figure 8.

Bearing in mind that the 2D $^{1}H-^{29}Si$ heteronuclear correlation experiment without LG cross-polarization is not quite selective, nevertheless it can provide useful qualitative data especially using short cross-polarization mixing time (1 ms). Although the presence of weak cross-peaks correlating Q^4 structure units with w-HB silanols (cf. Figure 9) does not provide direct evidence of mutual spatial proximity due to the limited selectivity of the experiment, these results indicate nonrandom distribution of w-HB and s-HB with respect to the Q^n structure units. This seems to support the finding that larger fraction of w-HB silanols surrounds Q^4 compared with Q^3 structure units. The regions of clusters of strongly hydrogen-bonded hydroxyls are instead formed at the surface composed by a majority of the Q^3 units (≡Si−OH) providing a suitable number of binding sites and surface geometry. The surface structures (probably cavities) partially containing fully condensed Q^4 units (≡Si−O−) which can be considered as defects of regular surface arrangement contain too low amount of silanol groups to form clusters of strongly hydrogen-bonded OH's. That is why around these surface sites composed of Q^3 and Q^4 units, clusters of weakly hydrogen-bonded OH's are located.

From analysis of a spin-diffusion process in the modified network **TE-DM 3-1** (the best fits are presented in Figure 7), it is clear that the size of domains of strongly and weakly hydrogen-bonded OH groups is approximately the same as that in the case of net silica network (ca. 1 and 2 nm, respectively). On the contrary, non-hydrogen-bonded silanols do not correlate to any other proton species, which indicates their magnetic and physical isolation. Methyls are in close contact with both types of clusters, confirming that the presence of a relatively small number of methyl units at the surface does not interrupt hydrogen-bonding network. The high

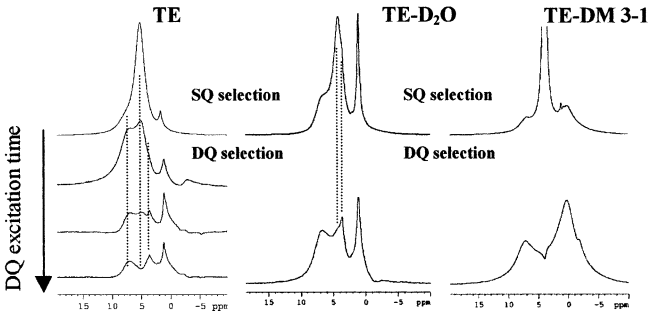

Figure 10. 1D double-quantum-filtered ^{1}H MAS NMR spectra of **TE**, **TE-D$_2$O**, and **TE-DM 3-1** measured by the C7 pulse sequence.

rate of equilibration of cross-peak intensity correlating methyls and strongly hydrogen-bonded OH's reflects their intimate mixing. The calculated size of dimethylsiloxane domains ca. 1 nm indicates that D^2 species occur in pairs that can be linked by Q^n structure units (see Figure 8). Significant interface was found between methyls and weakly hydrogen-bonded silanols. We propose that this interface reflects a portion of the methyl groups which are surrounded only by strongly hydrogen-bonded OH's. The resulting size of this interface is, however, an artifact of the computation method based on the model considering highly regular arrangement of the system. Similarly to the previous case, the clusters of strongly hydrogen-bonded protons are the predominant source of polarization of Q^3 structure units while the clusters of weakly hydrogen-bonded OH's were found around the sites composed of both Q^4 and Q^3 units (cf. Figure 9). From this 2D spectrum it is also clear that fully condensed Q^4 species link instead to D^2 units than to Q^3 species. This fact results from the increased reactivity of TEOS monomer units due to the copolymerization with DMDEOS monomers.

Double-Quantum-Filtered (DQF) ^{1}H MAS NMR. An interesting view of the order and molecular mobility of various OH protons and methyls is provided by DQF ^{1}H MAS NMR spectra. As there are no scalar couplings in the system, the presence of signals in DQF spectrum reflects dipolar couplings, which are static enough to produce pure double-quantum Hamiltonian. The efficiency of double-quantum selection and rate of buildup of DQ coherence reflect their strength.

The residual signal (ca. 5.2 ppm) of physisorbed water in DQF spectrum of hydrated system **TE** confirms a relatively high degree of organization of water molecules filling pores with suitable surface structure and size (cf. Figure 10). In general, liquid water is often described as having pseudocrystalline structure arising from short-range ordering of the water molecules into a hydrogen-bonded network. The short-range order of amorphous silica is also discussed in terms of similar models. These structural compatibilities for ordered water and silica then create the unique interfacial region. However, molecular motion and chemical exchange destroys DQ coherence at longer excitation times. The signal corresponding to non-hydrogen-bonded silanols directly indicates residual static dipolar interactions, which are effectively recoupled. Furthermore, non-hydrogen-bonded silanols cannot be considered as isolated units but instead as pairs. DQF ^{1}H MAS NMR spectrum of partially deuterated network **TE-D$_2$O** clearly revealed that signal of weakly hydrogen-bonded OH at ca. 3.5 ppm reflects both labile residual water molecules and immobilized OH groups. The signal of

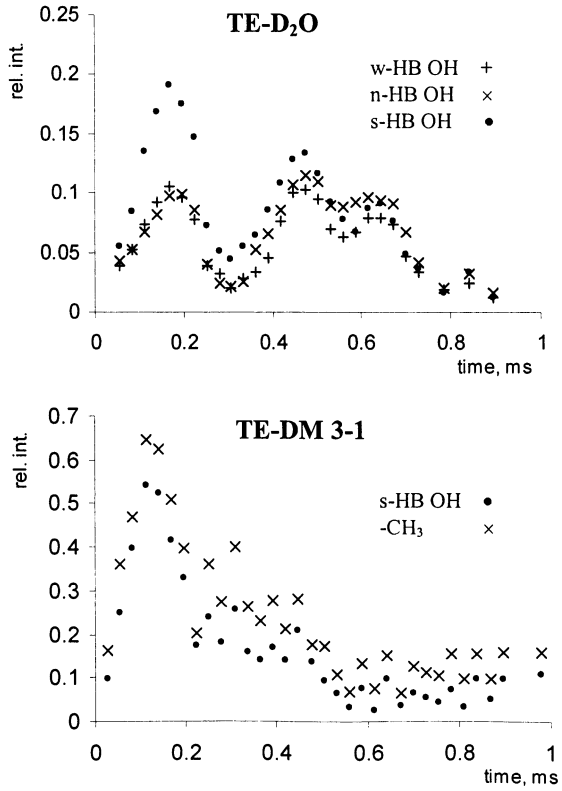

Figure 11. Dependences of double quantum filtration efficiency on excitation time (C7 pulse sequence was applied).

mobile water is attenuated by molecular motion during longer DQ excitation and reconversation, while the signal of immobilized hydroxyls is preserved. The oscillation of DQ built-up curves (see Figure 11) clearly indicates that dominant dipolar interactions occur in a weakly coupled and thus an effectively small number spin system with relatively well-defined geometry.[48] This follows from relatively high spinning speed (ca. 10 kHz) and predominant localization of protons at the surface. A higher efficiency of DQ selection of strongly hydrogen-bonded sites compared with weakly hydrogen-bonded hydroxyls nicely reflects their higher rigidity.

The DQ built-up curves obtained for modified system **TE-DM 3-1** clearly reflect multispin behavior. A much higher degree of excitation of DQ coherence of strongly hydrogen-bonded sites in this product compared with silica network **TE** corresponds to much stronger static dipolar couplings and thus to the tight spatial proximity of these hydroxyls to methyls. The faster coherence dumping out during excitation and reconversation time confirms a large number of mutually interacting spins, which are spatially close; however, their distance is not quite uniform. Interference of several couplings of different strengths leads to cancellation of oscillations, because different frequencies are destructively superimposed. In addition, higher spin correlation and multiple quantum coherences are also excited during longer excitation time in multibody spin system. Nevertheless, a high efficiency of the formation of pure double quantum Hamiltonian reflects secular interaction between strongly hydrogen-bonded hydroxyls (silanols and water) and methyls as is clearly reflected by the cross-peak in the 2D DQ ^{1}H MAS NMR spectrum (see Figure 12). The intensity of this signal reflects the fact that significant fraction of hydroxyls and methyls are involved in mutual interaction. This is the evidence that

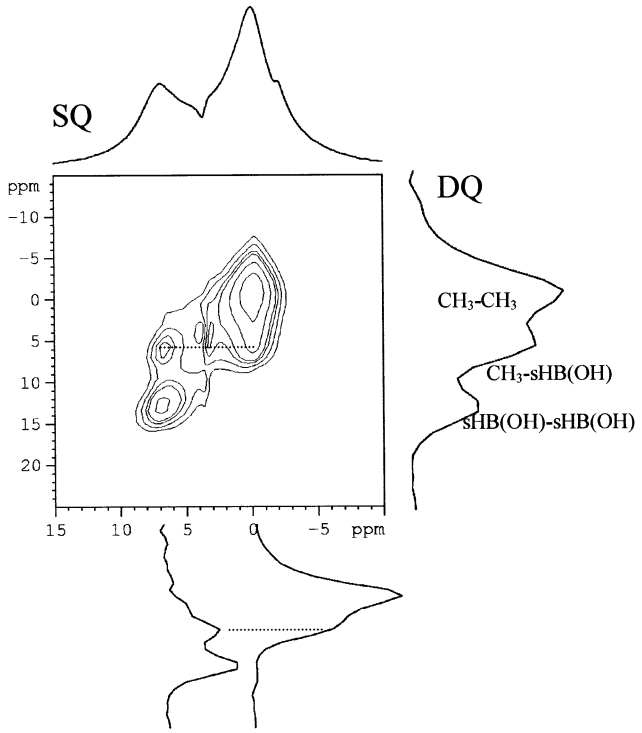

Figure 12. 2D DQ ^{1}H MAS NMR spectrum of the **TE-DM 3-1** system.

methyl groups are directly involved in the formation of strongly hydrogen-bonded clusters.

Conclusion

Various types of hydroxyls without fast chemical exchange were identified in fully hydrated silica network by ^{1}H CRAMPS experiments. Hydroxy protons are not involved in homogeneous hydrogen-bonding network and, instead, clusters of OH groups with different average hydrogen-bond strengths are formed. 2D ^{1}H CRAMPS spin-exchange experiments showed that almost all protons in pure silica network are mutually dipolar-coupled (their interatomic distance is not larger than 0.5 nm). In organically modified system, strong interaction between strongly hydrogen-bonded OH and methyl protons was confirmed by a 2D DQ ^{1}H MAS experiment. A significant fraction of methyl groups is directly involved in formation of hydrogen-bond network. The sizes of clusters of strongly and weakly hydrogen-bonded OH protons are <1 and $1-2$ nm, respectively. Non-hydrogen-bonded silanols and dimethylsiloxane units are present in pairs. Formation of cluster of OH protons with different strength of hydrogen bond is related to the arrangement of siloxane units of polysiloxane matrix. In the surface regions partially containing Q^4 units, clusters of weakly hydrogen-bonded OH's are formed, while regions predominantly consisting of surface silanol groups (Q^3) provide suitable binding sites to form clusters of strongly hydrogen-bonded protons. Quantum chemical geometry optimization of local structures of hydrogen-bonding sites and subsequent calculations of the ^{1}H NMR chemical shifts were used in the analysis of experimental data.

Acknowledgment. The authors thank the Grant Agency of the Czech Republic (Grant 203/98/P290) and the Grant Agency of Academy of Sciences of the Czech Republic (Grant K4050111) for financial support.

References and Notes

(1) Chuang, I. S.; Maciel, G. E. *J. Phys. Chem. B* **1997**, *101*, 3052.
(2) Kinney, D. R.; Chuang, I. S. Maciel, G. E. *J. Am. Chem. Soc.* **1993**, *115*, 6786.
(3) Changhua, C. L.; Maciel, G. E. *J. Am. Chem. Soc.* **1996**, *118*, 5103.
(4) Bronnimann, C. E.; Zeigler, R. C.; Maciel, G. E. *J. Am. Chem. Soc.* **1988**, *110*, 2023.
(5) d'Espinose de la Caillerie, J. B.; Aimeur, M. R.; Kortobi, Y. E.; Legrand, A. P. *J. Colloid Interface Sci.* **1997**, *194*, 434.
(6) Vega, A. J.; Scherer, G. W. *J. Non-Cryst. Solids* **1989**, *111*, 153.
(7) Turov, V. V.; Leboda, R.; Bogillo, V. I.; Skubiszevska-Zieba, J. *Langmuir* **1997**, *13*, 1237.
(8) Chuang, I. S.; Kinney, D. R.; Maciel, G. E. *J. Am. Chem. Soc.* **1993**, *118*, 8695.
(9) Baboneau, F. *New J. Chem.* **1994**, *18*, 1065.
(10) Maciel, G. E.; Sindorf, D. W. *J. Am. Chem. Soc.* **1980**, *102*, 7606.
(11) Sindorf, D. W.; Maciel, G. E. *J. Am. Chem. Soc.* **1981**, *103*, 4263.
(12) Sindorf, D. W.; Maciel, G. E. *J. Am. Chem. Soc.* **1983**, *105*, 1487.
(13) Sindorf, D. W.; Maciel, G. E. *J. Phys. Chem.* **1982**, *86*, 5208.
(14) Sindorf, D. W.; Maciel, G. E. *J. Am. Chem. Soc.* **1983**, *105*, 3767.
(15) Sindorf, D. W.; Maciel,, G.E. *J. Phys. Chem.* **1982**, *87*, 5516.
(16) Devreux, F.; Boilot, J. P.; Chaput, F.; Lecomte, A. *Phys. Rev. A* **1990**, *41*, 6901.
(17) Malier, L.; Devreux, F.; Chaput, F.; Boilot, J. P.; Axelos, M. A. V. *J. Non-Cryst. Solids* **1992**, *147*, 686.
(18) Chuang, I. S.; Maciel, G. E. *J. Am. Chem. Soc.* **1996**, *118*, 401.
(19) Stevens, N. S. M.; Rezac, M. E. *Polymer* **1999**, *40*, 4289.
(20) Fidalgo, A.; Nunes, T. G.; Ilharco, L. M. *J. Sol-Gel Sci. Technol.* **2000**, *19*, 403.
(21) Loy, D. A.; Baugher, B. M.; Bauugher, C. R.; Schneider, D. A.; Rahimian, K. *Chem. Mater.* **2000**, *12*, 3624.
(22) Brus, J.; Dybal, J. *Polymer* **2000**, *41*, 5269.
(23) Brus, J.; Skrdlantova, M. *J. Non-Cryst. Solids* **2001**, *281*, 61.
(24) Brus, J. *J. Sol-Gel Sci. Technol.* **2002**, *25*, 17.
(25) Baboneau, F.; Gualandris, V.; Maquet, J.; Massiot, D.; Janicke, M. T.; Chmelka, B. F. *J. Sol-Gel Sci. Technol.* **2000**, *19*, 113.
(26) Vega, A. J. *J. Am. Chem. Soc.* **1988**, *110*, 1049.
(27) Peeters, M. P. J.; Wakelkamp, W. J. J.; Kentgens, A. P. M. *J. Non-Cryst. Solids* **1995**, *189*, 77.
(28) Burum, D. P.; Rhim, W. K. *J. Chem. Phys.* **1979**, *71*, 314.
(29) Caravatti, P.; Neuenschwander, P.; Ernst, R. R. *Macromolecules* **1985**, *18*, 119.
(30) van Rossum, B. J.; Forster, H.; de Groot, H. J. M. *J. Magn. Reson.* **1997**, *124*, 516.
(31) Lee, Y. K.; Kurur, N. D.; Helmle, M.; Johansen, O. G.; Nielsen, N. C.; Levitt, M. H. *Chem. Phys. Lett.* **1995**, *242*, 304.
(32) Frisch, M. J.; Trucks, G. W.; Schlegel, H. B.; Scuseria, G. E.; Robb, M. A.; Cheeseman, J. R.; Zakrzewski, V. G.; Montgomery, J. A., Jr.; Stratmann, R. E.; Burant, J. C.; Dapprich, S.; Millam, J. M.; Daniels, A. D.; Kudin, K. N.; Strain, M. C.; Farkas, O.; Tomasi, J.; Barone, V.; Cossi, M.; Cammi, R.; Mennucci, B.; Pomelli, C.; Adamo, C.; Clifford, S.; Ochterski, J.; Petersson, G. A.; Ayala, P. Y.; Cui, Q.; Morokuma, K.; Malick, D. K.; Rabuck, A. D.; Raghavachari, K.; Foresman, J. B.; Cioslowski, J.; Ortiz, J. V.; Stefanov, B. B.; Liu, G.; Liashenko, A.; Piskorz, P.; Komaromi, I.; Gomperts, R.; Martin, R. L.; Fox, D. J.; Keith, T.; Al-Laham, M. A.; Peng, C. Y.; Nanayakkara, A.; Gonzalez, C.; Challacombe, M.; Gill, B.; Johnson, P. M. W.; Chen, W.; Wong, M. W.; Andres, J. L.; Gonzalez, C.; Head-Gordon, M.; Replogle, E. S.; Pople, J. A. Gaussian 98, Revision A.7. Gaussian, Inc.: Pittsburgh, PA, 1998.
(33) Becke, A. D. *J. Chem. Phys.* **1993**, *98*, 1372.
(34) Ditchfield, R. *Mol. Phys.* **1974**, *27*, 789.
(35) Cheesman, J. R.; Trucks, G. W.; Keith, T. A.; Frisch, M. J. *J. Chem. Phys.* **1996**, *104*, 5497.
(36) Robert, E.; Whittington, A.; Fayon, F.; Pichavant, M.; Massiot, D. *Chem. Geol.* **2001**, *174*, 291.
(37) Eckert, H.; Yesinowski, J. P.; Silver, L. A.; Stolper, E. M. *J. Phys. Chem.* **1988**, *92*, 2055.
(38) Brunner, E.; Sternberg, U. *Prog. Nucl. Magn. Reson. Spectrosc.* **1998**, *32*, 21.

(39) Fyfe, C. A.; Zhang, Y.; Aroca, P. *J. Am. Chem. Soc.* **1992**, *114*, 3252.
(40) Schaller, T.; Sebald, A. *Solid State Nucl. Magn. Reson.* **1995**, *5*, 89.
(41) Brus, J.; Petříčková H.; Dybal, J. *Solid State Nucl. Magn. Reson.* Submitted for publication.
(42) Schmidt-Rohr, K.; Spiess, H. W. *Multidimensional Solid-State NMR and Polymers*; Academic Press: New York, 1994.
(43) Clauss, J.; Schmidt-Rohr, K.; Spiess, H. W. *Acta Polym.* **1993**, *44*, 1.
(44) Brus, J.; Dybal, J.; Schmidt, P.; Kratochvíl, P.; Baldrian, J. *Macromolecules* **2000**, *33*, 6448.
(45) Brus, J.; Dybal, J.; Sysel, P.; Hobzová, R. *Macromolecules* **2002**, *35*, 1253.
(46) Assink, R. A. *Macromolecules* **1978**, *11*, 1233.
(47) Capitani, D.; Proietti, N.; Ziarelli, F.; Serge, A. L. *Macromolecules* **2002**, *35*, 5536.
(48) Schnell, I.; Spiess, H. W. *J. Magn. Reson.* **2001**, *151*, 153.

MA0204249